Development 139, 1987-1996 (2012) doi:10.1242/dev.076893

Stable and dynamic microtubules coordinately determine and maintain *Drosophila* bristle shape

Amir Bitan, Ido Rosenbaum and Uri Abdu*

SUMMARY

Within interphase cells, microtubules (MTs) are organized in a cell-specific manner to support cell shape and function. Here, we report that coordination between stable and dynamic MTs determines and maintains the highly elongated bristle cell shape. By following MT-decorating hooks and by tracking EB1 we identified two MT populations within bristles: a stable MT population polarized with their minus ends distal to the cell body, and a dynamic MT population that exhibits mixed polarity. Manipulating MT dynamics by *Klp10A* downregulation demonstrates that MTs can initiate new shaft extensions and thus possess the ability to determine growth direction. Actin filament bundling subsequently supports the newly formed shaft extensions. Analysis of *ik2* mutant bristles, established by elongation defects in the *Drosophila ikkε* homolog, led to the observation that stable and dynamic MT orientation and polarized organization are important for proper bristle elongation. Thus, we demonstrate for the first time that coordination between stable and dynamic MT sets that are axially organized yet differently polarized drives cell elongation.

KEY WORDS: Cell shape, *Drosophila*, Microtubule polarity

INTRODUCTION

Microtubules (MTs) are polarized structural elements that are vital for many cellular processes. One of the most addressed MT-dependent functions is the proper segregation of chromosomes during mitosis and meiosis. MTs also participate directly and indirectly in determining and maintaining the global organization of the cytoplasm and cell shape during interphase (Sawin and Nurse, 1998). Furthermore, the MT infrastructure supports intracellular movements, cell polarity determination and cell migration. Reflecting cell-specific requirements, interphase MTs can be organized in different manners.

The construction of long and polarized cells offers an opportunity to investigate how MTs organize and how their organization supports and drives cell elongation. In *Drosophila*, mechanosensory bristles are part of the peripheral nervous system and serve as rigid extensions of underlying sensory neurons (Lees and Waddington, 1942). The bristles are cone-shaped structures that can elongate up to 400 μm over the course of 16 hours, relying on actin polymerization and bundling for this purpose (Tilney et al., 2000). However, it has also been suggested that MTs play a role in such elongation (Fei et al., 2002). By tracking the localization pattern of a MT polarity reporter, we previously proposed that more than half of all bristle MTs are polarized, with their minus ends distal to the cell body. We also reported that proper MT organization in the bristle shaft is necessary for the asymmetric distribution of proteins and for proper cell elongation (Bitan et al., 2010a; Bitan et al., 2010b). However, it remained unknown how MT organization within the bristle shaft contributes to cell elongation and shape.

Department of Life Sciences and the National Institute for Biotechnology in the Negev, Ben-Gurion University, Beer-Sheva 84105, Israel.

*Author for correspondence (abdu@bgu.ac.il)

Accepted 19 March 2012

In this study, we demonstrate for the first time that bristle MTs are composed of two different MT sets. The first MT population comprises stable, minus end-distal unipolarized MTs. We suggest that these MTs serve as polarized tracks that allow the proper distribution of cellular components necessary for bristle elongation. The second MT population is dynamic and shows mixed polarity. Most importantly, we demonstrate by the reduction of dynamic MT catastrophe using Klp10A RNAi downregulation that dynamic MTs can initiate shaft extensions and hence possess the ability to determine polarity and affect bristle elongation. Actin filament bundling subsequently supports these shaft extensions so as to allow proper axial elongation. Based on analysis of bristle elongation defects demonstrated by mutants of the *Drosophila ikkε* homolog *ik2*, we report that stable and dynamic MT orientation and polarized organization are important for proper bristle elongation. Thus, our results show how stable and dynamic MTs cooperate to determine both bristle polarity and proper biased axial elongation of the bristle shaft.

MATERIALS AND METHODS

Drosophila stocks and developmental staging

The Oregon-R strain of *Drosophila melanogaster* served as the wild type in these studies. The following mutant and transgenic flies were used: pUAS ik2^{K41A} (Oshima et al., 2006), HA-Dhc64C (Silvanovich et al., 2003), pUAS GFP-EB1 (Satoh et al., 2008), pUAS Klp10A RNAi (Vienna *Drosophila* RNAi Center, V41534), pUAS GFP (Bloomington Stock Center, 6658) and pUAS DIAP1 (Kuranaga et al., 2002). Bristle expression was induced under the control of the *neur*-Gal4 driver. All animals were staged from the point of puparium formation (Bainbridge and Bownes, 1981). White prepupae were collected and placed on double-sided Scotch tape in a Petri dish that was placed in a 25°C incubator, as previously described (Tilney et al., 2000). To allow accurate analysis, all confocal images and data presented in this work were obtained from macrochaete bristles.

Live imaging

After removing the pupal case, pupae were glued using heptane glue thorax side down in a glass-bottom culture dish (MatTek). A press-to-seal silicone isolator (Invitrogen) was placed on the dish to allow water addition to the

periphery of the dish to achieve the proper conditions of humidity. Confocal images were taken on an Olympus FV1000 laser-scanning confocal microscope. For elongation tracking, *z*-stacks were acquired every 30 minutes. Time-lapse movies at eight frames per second were generated using ImageJ. Images for EB1-tracking time-lapse movies were acquired at intervals of 1936 mseconds.

EB1 tracking analysis

Owing to the long comet tails of GFP-EB1, we were unable to perform automatic tracking. Hence, tracking was performed manually using ImageJ to count the duration, start and end point of each EB1 track. These data were then analyzed using Matlab R2010b (MathWorks). Annotated images were generated using the Annotation function and rose diagrams were generated using the Rose function.

Bristle phalloidin and antibody staining

Procedures for bristle fixation and staining were as described previously (Bitan et al., 2010b; Guild et al., 2002). Mouse monoclonal anti-α-tubulin (1:250; Sigma), rat monoclonal anti-hemagglutinin (HA) (1:200; Roche), mouse monoclonal anti-acetylated tubulin (1:200; Sigma), rat monoclonal anti-YL1/2 tyrosinated tubulin (1:100; Sigma) and mouse monoclonal anti-Glu-α-tubulin (Synaptic Systems) primary antibodies were used. Cy3-conjugated goat anti-mouse (1:100; Jackson ImmunoResearch) and Cy3-conjugated goat anti-rat (1:100; Jackson ImmunoResearch) antibodies served as secondary antibodies. For actin staining, Oregon Green 488- or Alexa Fluor 568-conjugated phalloidin (1:250; Molecular Probes) was used.

Scanning electron microscopy (SEM)

Adult *Drosophila* were fixed and prepared for SEM as described (Bitan et al., 2010b). Samples were examined with a JEOL JSM 7400F scanning electron microscope.

MT-decorating hooks

The hook decoration procedure (McIntosh and Euteneuer, 1984) for *Drosophila* has been outlined in detail (Mogensen et al., 1989). Isolated thoraces were rinsed for 1 minute at 37°C in 0.5 M Pipes buffer pH 6.9 containing 1 mM EDTA, 1 mM $MgCl_2$ and 1 mM GTP, with or without 10 μM taxol. Thoraces were then extracted for 20 minutes at 37°C in the same 0.5 M Pipes buffer also containing 1% Triton X-165, 0.5% sodium deoxycholate, 0.02% SDS, 3.5% DMSO, with or without 10 μM taxol. The samples were then rinsed twice for 1 minute each in the same buffer and then incubated for 5 minutes at 4°C in 0.5 M Pipes buffer pH 6.9 containing 3.5% DMSO, 1 mM $MgCl_2$, 1 mM EDTA, 1 mM GTP and 2 mg/ml bovine brain tubulin (Cytoskeleton) followed by a 1-hour incubation at 37°C. Samples were then fixed for transmission electron microscopy.

Transmission electron microscopy (TEM)

Freshly isolated thoraces or thoraces after hook decoration treatment were fixed for TEM as described (Tilney et al., 1998). Samples were fixed in 2% glutaraldehyde (Electron Microscope Sciences) in 0.05 M phosphate buffer pH 6.8 for 10 minutes at room temperature followed by a 1-hour fixation on ice in 1% glutaraldehyde, 1% OsO_4 in 0.05 phosphate buffer pH 6.2. After fixation, samples were washed three times over 1 hour total in cold water (4°C), followed by overnight staining with 1% uranyl acetate at 4°C. Thoraces were then dehydrated in a series of 15-minute acetone rinses (30, 50, 70, 80, 90, 100, 100%), followed by two 15-minute rinses in propylene oxide, 1 hour in 2:1 propylene oxide:araldite, overnight incubation in 1:1 propylene oxide:araldite and 1 hour in araldite. Each thorax was then placed on an embedding plate in a 60°C oven overnight. Thin longitudinal or transverse sections were cut with a diamond knife in a microtome. Since MT hooks are asymmetric, it was important to know the viewing direction of each transverse section. Therefore, for hook-decorated specimens, the block was molded asymmetrically prior to cutting and all sections were generated and collected on grids in the same orientation. Sections were mounted on 100 mesh copper grids coated with formvar, stained with uranyl acetate and lead citrate and examined with an electron microscope (FEI Tecnai 12). In each bristle transverse section, all MTs were counted and divided into three groups: clockwise hooks, counter-clockwise hooks and ambiguous.

For bristle longitudinal sections, each MT was tracked manually using ImageJ and was represented by two points, assuming that MTs form straight lines. A reference line representing the axis of the shaft was drawn and MT angles relative to this line were calculated using Matlab R2010b, and annotated images and rose diagrams generated as described above.

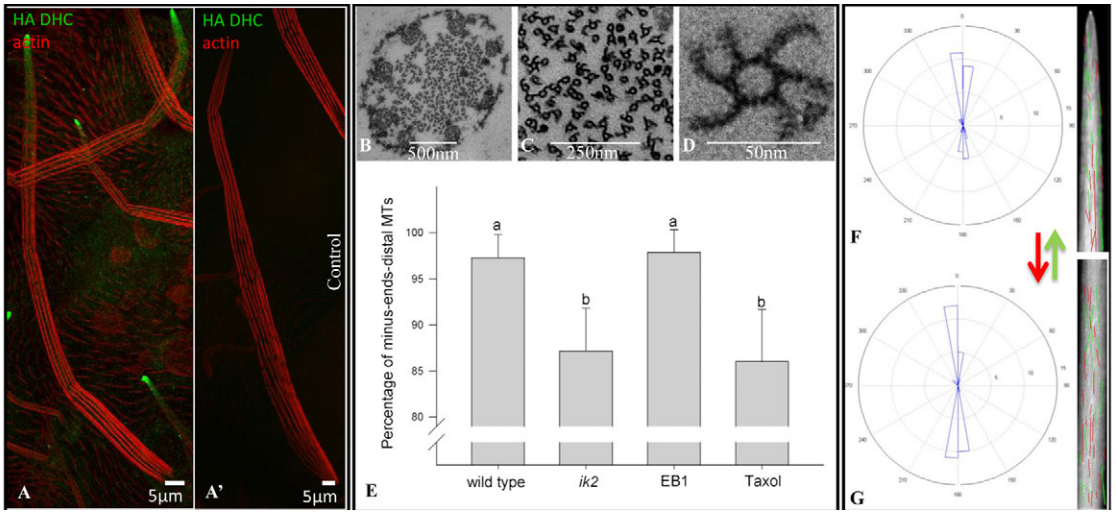

Fig. 1. MT polarity in elongating bristles. (**A**) Confocal projection of an elongating bristle expressing HA-tagged dynein heavy chain (DHC) under its endogenous promoter, stained with anti-HA antibodies (green) and phalloidin (red). Dynein heavy chain is enriched at the bristle tip. (**A′**) Control image of an elongating wild-type bristle, stained with anti-HA antibodies (green) and phalloidin (red). (**B-D**) TEM micrographs at increasing magnification of thin transverse sections through a microchaete from a thorax treated to induce the formation of MT-decorating hooks before fixation. (**E**) MT-decorating hooks analysis in wild-type, *ik2*, GFP-EB1 and taxol-treated thoraces. Mean±s.d. Minus end-distal MTs were more prevalent in wild-type and EB1 populations than among *ik2* and taxol-treated populations (nested ANOVA, $F_{3,18}$=30.37, P<0.001; Tukey's post-hoc test, P<0.001). Differences between individual flies were not significant ($F_{18,46}$=1.24, P=0.275). Lowercase letters (a and b) indicate groups that are significantly different. (**F**,**G**) Tracking of the MT plus-end dynamics reporter GFP-EB1 (*neur*-Gal4; pUAS GFP-EB1) in elongating bristle tip (F, see also supplementary material Movie 1, part A) and middle shaft (G, see also supplementary material Movie 1, part B) regions. Red lines indicate base-directed tracks and green lines indicate tip-directed tracks. Rose diagrams of EB1 track angles relative to the axis of the shaft show bi-directional EB1 movement.

Statistical analysis

For MT-decorating hook experiments, we compared the populations of minus end-distal MTs from wild type and the various treatments/genotypes using a nested ANOVA model (individual thoraces nested within treatments), followed by Tukey's post-hoc test. The proportion data were arcsine transformed. MT densities within each section were compared using the Mann-Whitney U test. For MT degree dispersal analysis, we compared wild-type tips and lower shafts with *ik2* mutant swollen areas and lower shafts. Angles were divided into categories of 0-30°, 30-60° and 60-90°, and their distributions were compared within and between treatments using Pearson's χ^2 test. EB1 tracks were divided into tip- or base-directed movements, with distribution also being compared using Pearson's χ^2 test. Data are presented as mean±s.d.; *n* represents the number of MTs. All statistical analyses were conducted using Statistica version 8.0 (Statsoft).

RESULTS

The bristle cytoplasm is enriched with minus end-distal MTs

In our previous work, we found that the MT minus end-directed reporter Nod:KHC is concentrated at the bristle tip (Bitan et al., 2010b). Since Nod:KHC is a synthetic chimeric protein, we tested the localization pattern of the minus end-directed motor dynein. We found that the dynein heavy chain was also concentrated at the bristle tip (Fig. 1A). Taking into consideration that MTs form short overlapping polymers rather than being stretched along the length of the shaft (Tilney et al., 2000), these findings led us to assume that the majority of bristle MTs would be polarized, with their minus ends distal to the cell body to allow such tip concentration. To investigate MT polarity at single MT resolution within a bristle, we used the MT-decorating hooks technique in which high-molarity Pipes buffer promotes tubulin assembly onto asymmetrically hook-shaped appendages present on pre-existing MT proto-filaments (McIntosh and Euteneuer, 1984). Hook direction, i.e. clockwise or counter-clockwise, indicates the polarity orientation of the parent MT. Thin transverse sections through thoraces that were treated to induce the formation of MT-decorating hooks before fixation were analyzed for hook direction. We found that 97±2.5% (mean±s.d., *n*=5211 MTs) of bristle MTs were polarized with their minus ends distal to the cell body (Fig. 1B-E). Differences between individual flies were not significant ($F_{18,46}$=1.24, *P*=0.275) using a nested ANOVA model (individual flies nested within treatments).

Tracking EB1 in elongating bristles reveals a second, distinct population of MTs in the shaft with mixed polarity

To identify growing MTs and to track their polarity within the elongating shaft, we followed the End-binding protein (EB1), which binds to the dynamic plus ends of MTs (Baas and Lin, 2011). Using the Gal4/UAS expression system, we expressed GFP-EB1 in bristles and tracked EB1 movement after shaft initiation in pupae older than 32 hours after puparium formation (APF). In elongating bristles (32-48 hours APF), EB1 formed straight comet-like tracks along the entire shaft that led with their brightest part, meaning that EB1 tracks moved in the MT plus-end direction. To our surprise, directional analysis of the EB1 tracks revealed bi-directional movements indicative of mixed polarity MTs that polymerize or that move within the shaft. These movements were almost parallel to the axis of the shaft, with 76±6% (*n*=331) of EB1 tracks being oriented within 30° of the axis of the shaft (Fig. 1F,G), favoring the tip direction near the tip (68±8%) (Fig. 1F and supplementary material Movie 1, part A), yet revealing no significant preference of direction in the rest of the shaft (40±6% tip-directed tracks) (Fig. 1G and supplementary material Movie 1, part B). No significant differences in angle distribution were found within the wild-type bristles examined (χ^2_6=2.85, *P*=0.827 for the tip region and χ^2_6=3.6, *P*=0.731 for middle and base segments).

We were intrigued by this EB1 bi-directionality, which signals a bipolar MT organization, given that examination of the MT-decorating hooks indicated an almost unipolar organization of MTs in the shaft. To test for the possibility that overexpression of EB1 in bristles altered the normal distribution of MT polarity, we performed the MT-decorating hooks assays on GFP-EB1-expressing flies. To our surprise, we found that, as in wild-type flies, 97.8±2.4% (*n*=2389) of GFP-EB1-expressing bristle MTs were polarized, with their minus ends distal to the cell body and with no indication of the bipolar organization implied upon tracking GFP-EB1 movement in elongating bristles. No significant differences were found between the wild-type and EB1 populations (Tukey's post-hoc test, *P*=0.829) (Fig. 1E).

In addition, SEM of adult GFP-EB1-expressing bristles revealed bristles with no morphological defects (see Fig. 4C), indicating that overexpression of GFP-EB1 had no noticeable effect on normal bristle elongation. Since EB1 binds to growing and hence more dynamic MTs, it is plausible that these MTs

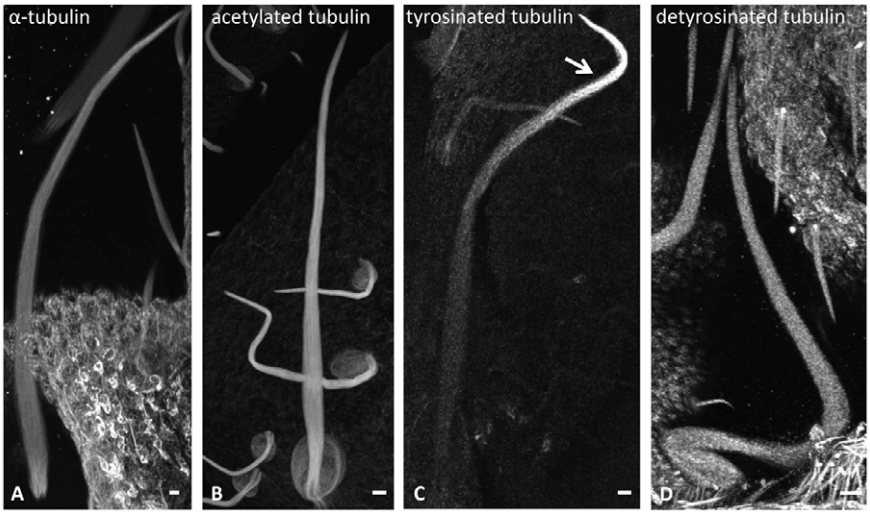

Fig. 2. MTs in the shaft are composed of dynamic and stable subpopulations. (**A-D**) Confocal projections of elongating bristles stained with (A) anti-α-tubulin, (B) anti-acetylated tubulin, (C) anti-tyrosinated tubulin and (D) anti-de-tyrosinated tubulin antibodies. Newer MTs are concentrated at the tip region (C, arrow), whereas older MTs (B,D) are dispersed along the shaft. Scale bars: 5 μm.

could be more vulnerable to the hooking and fixation procedures employed in our assay. To reduce this effect, we incubated the dissected thoraces with 10 μM taxol, an MT-stabilizing drug, during the extraction phase of the MT-decorating hooks technique. Stabilizing dynamic MTs using taxol should increase MT density in the bristle. However, because MT densities vary between bristles of the same genotype and even between bristles from the same pupa, as calculated by us and as also reported by Tilney et al. (Tilney et al., 2000), we were not surprised to find non-significant differences between the MT densities of taxol-treated and untreated thoraces (Mann-Whitney, U20,5=33, Z=1.15, P=0.248). However, the addition of taxol to the MT-decorating hooks procedure enabled us to preserve more of the dynamic MTs and resulted in 84.9±5.4% (n=1967) MTs that were polarized with their minus ends distal to the cell body, as compared with 97% in untreated thoraxes. This ~12% shift was found to be significant (Tukey's post-hoc test, P<0.001; Fig. 1E) and probably represents dynamic MTs that are polarized plus end distal. This finding also points to the existence of two MT populations in the shaft, one being a dynamic MT population that exhibits mixed polarity and the second comprising unipolarized minus end-distal MTs.

Two MT populations are revealed upon assessing post-translational modifications of tubulin in the shaft

To study the dynamic nature of the MT networks within the bristle shaft, we used different markers that report on the post-translational modifications of tubulin. In most eukaryotes, tubulin subunits are subject to post-translational modifications (Perdiz et al., 2011; Rosenbaum, 2000). Two of these modifications are de-tyrosination, whereby a conserved C-terminal tyrosine residue in the α-tubulin subunit is removed, and acetylation, which occurs on a single lysine residue (Rosenbaum, 2000). De-tyrosination and acetylation characterize aged and hence more stable MTs, whereas highly dynamic MTs contain tyrosinated tubulin (Ikegami and Setou, 2010; Rosenbaum, 2000). In elongating macrochaete bristles, we found that whereas α-tubulin, de-tyrosinated and acetylated tubulin are abundant along the entire shaft, tyrosinated tubulin is found in a gradient at the tip (Fig. 2). This gradient was even more prominent than the EB1 gradient in elongating bristles expressing GFP-EB1 (see Fig. 5J). These results strengthen those described above that indicate the presence of two MT populations in the bristle shaft, namely a stable population that fills the shaft and a younger, more dynamic MT population that is enriched toward the tip.

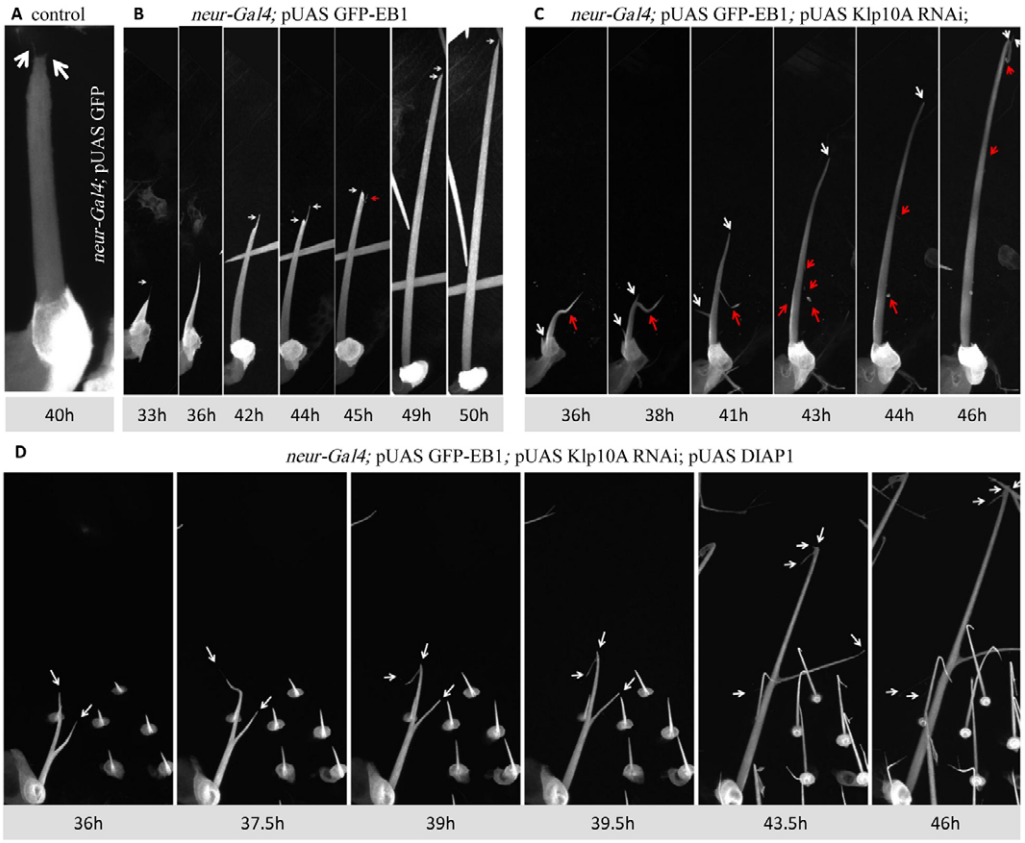

Fig. 3. Dynamic MTs determine shaft polarity and initiate shaft extensions. Time-lapse confocal projections of elongating posterior scutellar bristles. (**A**) Control bristle expressing GFP demonstrating tip extensions (arrows). (**B**) Bristles expressing GFP-EB1 (*neur*-Gal4; pUAS GFP-EB1) elongate axially. Elongation is led by a single extension that is always found at the tip (arrows). Where a new extension appears (white arrows), the preceding extension deforms (red arrows). See also supplementary material Movie 2. (**C**) Bristles co-expressing GFP-EB1 and Klp10A RNAi (*neur*-Gal4; pUAS GFP-EB1; pUAS Klp10A RNAi) also elongate axially. However, shaft extensions, which in wild-type bristles were restricted to the tip area, appear along the shaft in the mutant bristle (arrows). Eventually, only tip extensions prevail (white arrows), whereas other extensions deform (red arrows). See also supplementary material Movie 3, part A. (**D**) Bristles expressing GFP-EB1, Klp10A RNAi and DIAP1 (*neur*-Gal4; pUAS GFP-EB1; pUAS Klp10A RNAi; pUAS DIAP1). As with Klp10A RNAi bristles, shaft extensions, which in wild-type flies were restricted to the tip area, appear along the shaft in the mutant (arrows). However, the majority of these ectopic extensions do not deform during elongation. See also supplementary material Movie 3, part B. Time points are represented in hours after pupae formation.

Dynamic MTs determine shaft polarity and initiate shaft extension

To elucidate the importance of dynamic MTs in polarized bristle growth, we took a genetic approach to affecting MT dynamics in the shaft. Klp10A (Kinesin-like protein at cytological region 10A), a member of the *Drosophila* kinesin-13 family of proteins that serve as effectors of MT dynamics, depolymerizes kinetochore MTs at their minus ends to allow MT poleward flux (Rogers et al., 2004). RNAi knockdown of Klp10A alters MT dynamics by increasing the MT pause state and reducing the catastrophe rate (Mennella et al., 2005). To affect bristle MT dynamics, we downregulated Klp10A by RNAi in bristles and tracked bristle elongation using EB1 as a reporter of the dynamic MT population in the shaft. Wild-type bristles expressing GFP-EB1 began to elongate 32 hours APF (Fig. 3B and supplementary material Movie 2). At this point, a single shaft extension decorated the tip, indicating the growth direction. Shaft extensions at bristle tips have been described previously (Bitan et al., 2010b) and were also seen in control bristles expressing GFP (Fig. 3A). As the shaft elongated, wherever a new extension appeared, the preceding extension deformed (Fig. 3B and supplementary material Movie 2). Elongation ends with a single shaft that then begins cuticle secretion to form the mature bristle, which tapers into the bristle tip and is decorated with straight ridges (Fig. 4A,G).

Bristles co-expressing GFP-EB1 and Klp10A RNAi also initiate elongation with a single tip extension (Fig. 3C and supplementary material Movie 3, part A). However, rather early during shaft elongation new shaft extensions appear that are not restricted to the tip area (Fig. 3C and supplementary material Movie 3, part A, white arrows). These newly formed extensions elongate along with the main shaft. Later, during bristle elongation, the extra shaft extensions separate from the cell body by developing constrictions and swellings (Fig. 3C, time points 36-41 hours APF, and supplementary material Movie 3, part A), leaving blebs of GFP that are absorbed, similar to neuron pruning during *Drosophila* metamorphosis (Williams and Truman, 2005). Eventually, as the shaft elongates to its final length, ectopic extensions remain only at the tip. Mature bristles exhibit only vague remnants of these events and are characterized by minor defects in tip morphology (Fig. 4E,H). Ectopic shaft extensions during bristle elongation in Klp10A RNAi bristles also appear without overexpression of EB1 (Fig. 5E, arrows). Taken together, it appears that by reducing the MT catastrophe rate, we disrupted proper polarity determination in the shaft and enabled the generation of ectopic shaft extensions containing dynamic MTs, as represented by EB1.

Actin bundles are necessary to support and maintain shaft extensions

It has been suggested that bristle shaft formation initiates with a microvillar-like structure that represents the first stage in the morphogenesis of large actin bundles, and that only those formations that contain stable, tightly packed actin bundles prevail (Tilney et al., 2004). When stained with phalloidin to detect actin bundles, GFP-EB1-expressing bristles exhibited parallel actin bundles that were organized in modules along the entire shaft periphery (Fig. 5A). In these bristles, actin bundles were only absent at the edge of the bristle tip, which contained dynamic MTs, as represented by EB1 (Fig. 5A, arrow). However, although dynamic MTs represented by EB1 were present in the entire shaft and in all shaft extensions of bristles co-expressing GFP-EB1 and Klp10A RNAi (Fig. 5B), actin bundles were present only in what appeared to be the main shaft and were missing from the upper segment of the bristle and its extensions (Fig. 5C,D). These results indicate that, with respect to bristle shaft initiation, shaft extensions also need to be supported by actin bundles to prevail.

The existence of acetylated MTs in ectopic shaft extensions does not contribute to extension durability

To examine whether Klp10A RNAi-induced shaft extensions are composed solely of dynamic MTs, we stained elongating bristles co-expressing GFP-EB1 and Klp10A RNAi with anti-acetylated tubulin

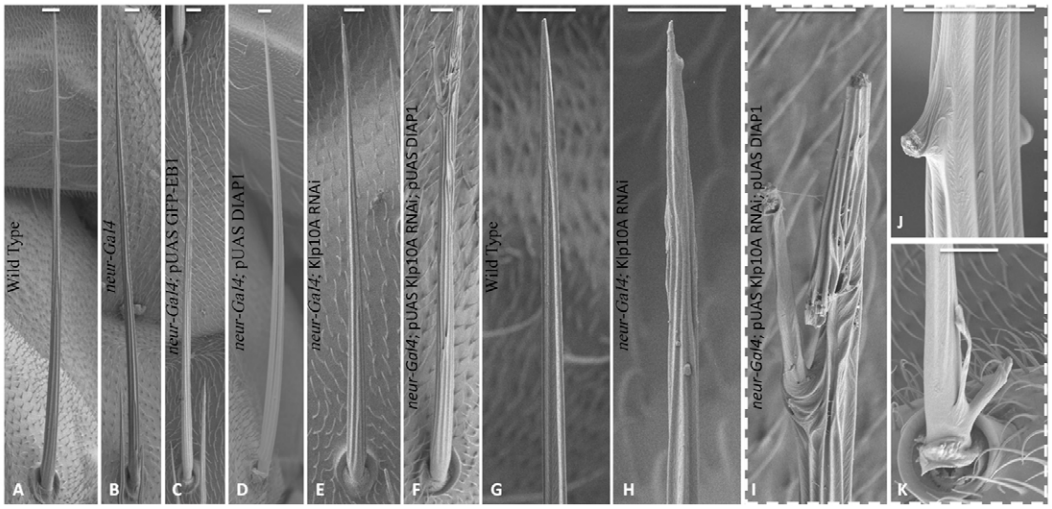

Fig. 4. Altering MT dynamics affects bristle morphology. (**A-K**) SEM of posterior dorsocentral bristles taken from wild-type flies (A and tip enlargement in G) and flies expressing Neur-Gal4 (B), GFP-EB1 (C), DIAP1 (D) and Klp10A RNAi (*neur*-Gal4; pUAS Klp10A RNAi) (E and tip enlargement in H) in the bristles and flies expressing Klp10A RNAi and overexpressing DIAP1 in the bristles (*neur*-Gal4; pUAS Klp10A RNAi; pUAS DIAP1) (F and enlargements in I-K). Klp10A RNAi bristles taper normally and reach the length of wild-type bristles (E) but end with an aberrant tip morphology characterized by smooth ridges and ectopic shaft extensions (H). Overexpression of DIAP1 with RNAi downregulation of Klp10A enhances the aberrant shaft extension phenotype seen in RNAi downregulation of Klp10A (H), resulting in multiple tips (I). In 37% of cases (n=16), ectopic shaft extensions were seen in the mid-shaft (J) or base (K) regions. Scale bars: 10 μm.

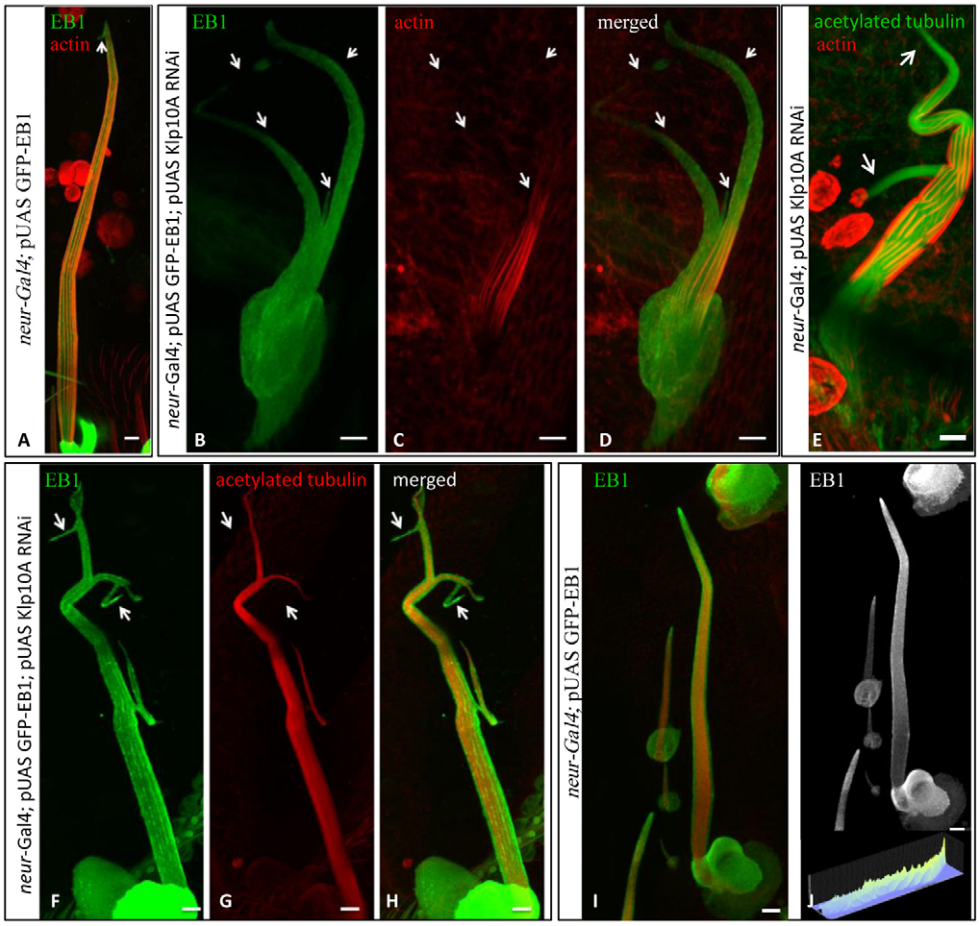

Fig. 5. Klp10A RNAi-induced shaft extensions do not contain actin or acetylated tubulin. (**A-J**) Confocal projections of elongating bristles expressing GFP-EB1 (*neur*-Gal4; pUAS GFP-EB1) (A,I,J) or Klp10A RNAi (*neur*-Gal4; pUAS Klp10A RNAi) (E) or co-expressing GFP-EB1 and Klp10A RNAi (*neur*-Gal4; pUAS GFP-EB1; pUAS Klp10A RNAi) (B-D,F-H), stained with phalloidin (red) (A,C-E) or anti-acetylated tubulin antibodies (E,G-I). In GFP-EB1-expressing bristles (A,I,J), EB1 is present along the entire shaft in a gradient at the tip (J, see intensity profile), whereas actin bundles are found along the shaft and are missing only in the restricted area of the growing tip (A, arrow). In bristles co-expressing GFP-EB1 and Klp10A RNAi (B-D), EB1 is found both in the shaft and the extensions, whereas actin bundles are found only in the lower part of the shaft (arrows). Ectopic shaft extensions are also present in bristles expressing Klp10A RNAi without overexpression of EB1 (E, arrows). In bristles co-expressing GFP-EB1 and Klp10A RNAi (F-H), acetylated tubulin is missing from some of the shaft extensions (F-H, arrows), in contrast to control bristles expressing only GFP-EB1, in which acetylated tubulin is found along the entire shaft. Scale bars: 5 μm.

antibodies. Whereas dynamic MTs, as represented by EB1, are present throughout the shaft and all its extensions, acetylated MTs are present in the main shaft and in only part of the extensions (Fig. 5F-H). These results indicate that the composition of MT populations within the shaft and extensions differ and that the presence of acetylated MTs in Klp10A RNAi-induced shaft extensions does not contribute to the durability of these extensions, as ectopic shaft extensions are missing in Klp10A RNAi mature bristles.

DIAP1 overexpression delays ectopic shaft extension pruning

The formation of shaft extensions and the subsequent absorbance of non-leading extensions observed in wild-type and Klp10A RNAi elongating bristles resemble larval dendrite pruning. Pruning is regulated by caspase activity, which is preceded by MT depolymerization and followed by cytoplasmic blebbing and degeneration (Kuo et al., 2006; Williams and Truman, 2005). It has been reported that *Drosophila* inhibitor of apoptosis protein 1 (DIAP1; Thread – FlyBase) inhibits caspases through direct binding or degradation (Kuranaga et al., 2006). Moreover, DIAP1 degradation leads to caspase activation and pruning, and DIAP1 stabilization interferes with this process (Rumpf et al., 2011). We therefore examined whether DIAP1 expression affected shaft extension absorbance in a manner similar to its affect on dendrite pruning.

Overexpression of DIAP1 had no visible effect on mature bristles (Fig. 4D). However, DIAP1 overexpression together with Klp10A RNAi downregulation enhanced the aberrant shaft extension phenotype of Klp10A RNAi mature bristles (Fig. 4I-K). Tracking the elongation of bristles expressing GFP-EB1 together with Klp10A RNAi and DIAP1 revealed that, as in Klp10A RNAi bristles, shaft extensions appeared ectopically along the shaft. However, the majority of these ectopic extensions did not deform during elongation and were visible throughout the elongation period (Fig. 3D and supplementary material Movie 3, part B). In mature bristles, ectopic shaft extensions were restricted to Klp10A RNAi bristle tips (Fig. 4E,H), whereas in bristles overexpressing DIAP1 together with Klp10A RNAi 37% of cases (from 16 macrochaete bristles examined) showed ectopic extensions that were abundant throughout the shaft (Fig. 4F,I-K).

Properly oriented MTs are necessary for polarized bristle growth

To better understand the importance of properly oriented MTs in shaft polarization, we searched for mutants exhibiting bristle polarization defects that were also reported to affect MTs. Ik2, which is encoded by the *Drosophila ikkε* homolog, is a member of the IκB kinase (IKK) family (Dubin-Bar et al., 2008; Shapiro and Anderson, 2006). Our previous work demonstrated that *ik2* affects MT organization in elongating bristles, ultimately affecting bristle shape (Bitan et al., 2010a; Bitan et al., 2010b). We now monitored the growth of *ik2* mutant bristles, using GFP-EB1 as a reporter of both dynamic MTs in the shaft and for the shaft borders. We found that *ik2* bristles initiate with a swollen area that moved upwards as the lower shaft elongated (Fig. 6A and supplementary material Movie 4, part A), and not with a single shaft extension, as is the

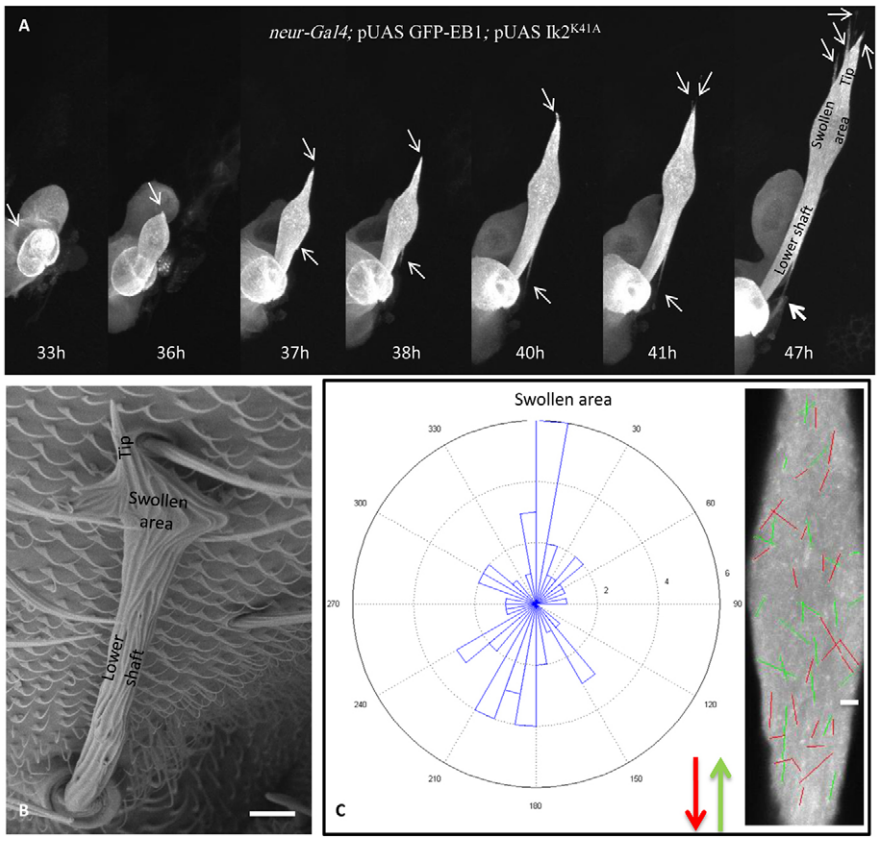

Fig. 6. In *ik2* mutant bristles, normal tip growth is blocked by an area containing disoriented dynamic MTs. (**A**) Time-lapse confocal projections of elongating posterior scutellar bristles of flies expressing the *ik2* dominant-negative form in the bristle and GFP-EB1 (*neur*-Gal4; pUAS GFP-EB1; pUAS ik2^{K41A}). In contrast to wild-type bristles (see Fig. 3B), *ik2* mutant bristle elongation initiates with a swollen area. This area moves upward as the lower shaft elongates and several persisting extensions form from this region (A, arrows). See also supplementary material Movie 4, part A. (**B**) SEM micrograph of bristles expressing the *ik2* dominant-negative form (*neur*-Gal4; pUAS ik2^{K41A}). The adult bristle (like the elongating bristle, A) is characterized by a long lower shaft and a swollen upper segment, which is in turn characterized by several extensions originating from this swollen region. (**C**) Tracking GFP-EB1 in bristles expressing the *ik2* dominant-negative form (*neur*-Gal4; pUAS GFP-EB1; pUAS ik2^{K41A}). In the swollen area, EB1 tracks are no longer oriented along the axis of the shaft but instead point in all directions. See also supplementary material Movie 4, part B. Red lines indicate base-directed tracks and green lines indicate tip-directed tracks. Time points are represented in hours after pupae formation. Scale bars: 10 μm in B; 2 μm in C.

case in wild-type flies (Fig. 3B). This swollen area did not appear to elongate, although extensions formed from this region (Fig. 6A and supplementary material Movie 4, part A).

ik2 mature bristles are thicker and shorter than wild-type bristles and are composed of a lower shaft that appears relatively normal, a swollen area that is characterized by disorganized ridges and is the widest part of the shaft, and a tip that presents multiple shaft extensions (Fig. 6B). Tracking GFP-EB1 in these bristles reveals that, in the swollen area only, 52±4% (n=118) of EB1 tracks were oriented within 30° of the bristle axis, while the rest of the EB1 tracks pointed in all directions (Fig. 6D and supplementary material Movie 4, part B). Angle distribution was significantly more diverse in the swollen area of the *ik2* mutants as compared with the wild-type tip region (χ^2_2=21.8, P<0.001), whereas no significant difference in the angle distribution was found for the lower shaft regions of wild-type and *ik2* bristles (χ^2_2=0.104, P=0.949). Directional analysis of *ik2* EB1 tracks revealed 53±4% tip-directed movements, a significant difference from the wild type (χ^2_1=8.67, P=0.003), whereas movements in the *ik2* lower shaft were not significantly different from those observed in wild-type lower shafts (χ^2_1=1.75, P=0.186). These results indicate that dynamic MTs were poorly oriented only in the swollen area of *ik2* bristles. No significant difference in the angle distribution was found when comparing individual *ik2* bristles (χ^2_2=1.23, P=0.542 for the swollen area; χ^2_4=6.57, P=0.160 for the lower shaft).

To ascertain how stable MTs were oriented in these bristles, we analyzed their orientation in TEM micrographs of thin longitudinal sections through microchaete bristles expressing the dominant-negative form of *ik2*. Rose diagram analysis of MT orientation in these micrographs revealed that in wild-type bristles, under the same fixation conditions, stable MTs ran parallel to the axis of the shaft (in the range of ±30°) in the base (98±0.48%, n=701), mid-shaft (99±0.78%, n=580) and tip (100%, n=66) regions (Fig. 7). By contrast, in *ik2* mutant bristles, stable MTs were highly disoriented (in the range of ±90°) and their angle distribution was significantly more diverse in the swollen area and tip of *ik2* mutant bristles as compared with the wild type (χ^2_2=18, P<0.001 for the tip region; χ^2_2=255, P<0.001 for the swollen area). In the swollen area, 62.18±4.28% (n=616) of MT angles were in the range of ±30°, whereas in the tip region 77±6.16% (n=162) of MT angles were in the range of ±30° (n=162) (Fig. 8).

Next, we analyzed thin traverse sections of various parts of the microchaete bristles from four different *ik2* mutant thoraces that were treated to induce the formation of MT-decorating hooks before fixation, without addition of taxol. We found that 87±4.6% (n=4902) of *ik2* mutant bristle MTs were polarized with their minus ends distal to the cell body, indicating a significant 10% difference from the wild type (Tukey's post-hoc test, P<0.001) (Fig. 1E). Differences between individual *ik2* mutant thoraces were not significant ($F_{18,46}$=1.24, P=0.275).

Together, these results indicate that both stable and dynamic MTs are disoriented in the tip and swollen areas of *ik2* mutant bristles that exhibit cell shape defects.

DISCUSSION

In this work, we demonstrate the existence of two different MT sets in the bristle shaft: a stable unipolarized MT population and a dynamic MT population that exhibits mixed polarity. This is the first reported case of two MT sets within the same cell exhibiting different polarities when tracked by EB1 or when hooked. This concept is important because in the few reported studies relying on both hooking and EB1 to estimate MT polarity within the cell, the

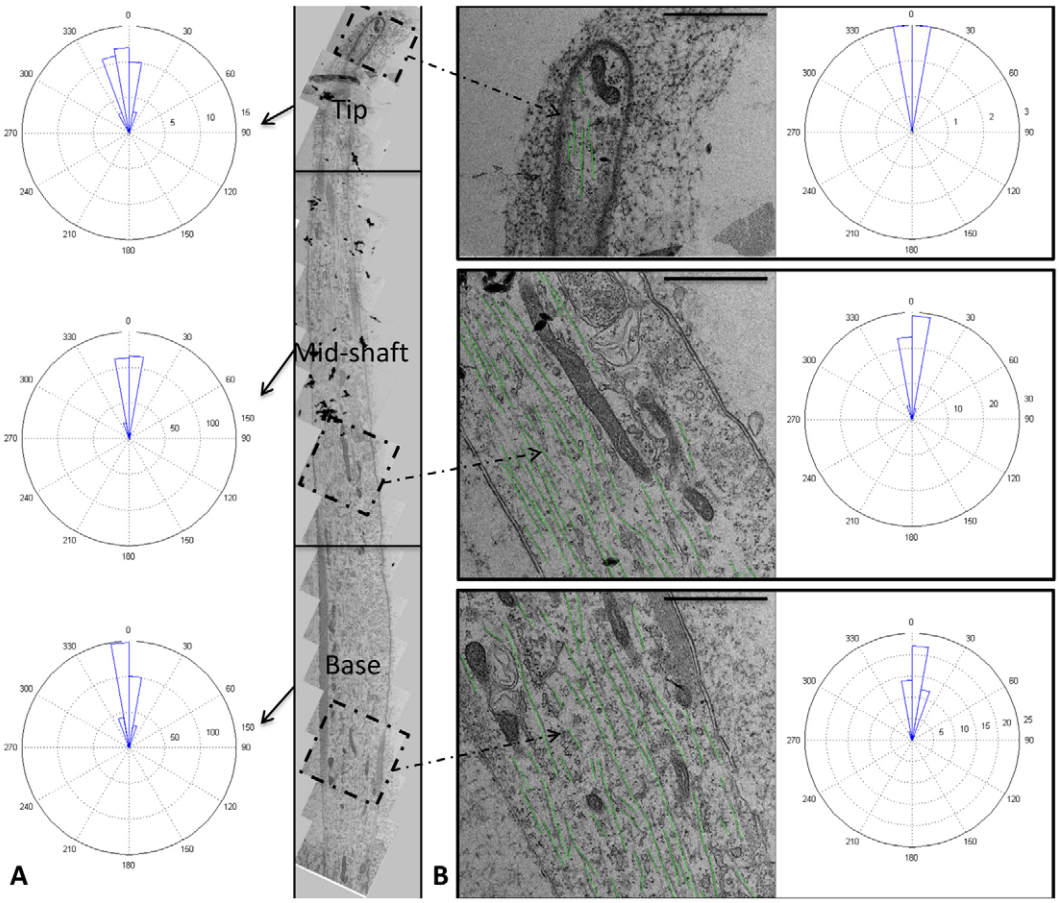

Fig. 7. Stable MTs run parallel to the axis of the wild-type bristle shaft. (**A**) TEM micrographs of thin longitudinal sections through microchaetes of wild-type flies and rose diagrams of all stable MT orientations relative to the axis of the shaft in the different bristle regions. (**B**) Representative micrographs and corresponding stable MT orientation rose diagrams. Wild-type stable MTs are parallel to the axis of the shaft (in the range ±30°). Green lines indicate detected MTs. Scale bars: 1 μm.

observed polarity was always the same (Baas and Lin, 2011). Moreover, in most studies, only one of these methods was used, probably under the mistaken assumption of their redundancy.

Given the presence of two distinct MT populations within bristles, we questioned the contribution of each pool to cell elongation. Since RNAi downregulation of Klp10A was reported to reduce MT catastrophe rates and extend the time period that MTs spend in the pause state (Mennella et al., 2005), we hypothesized that if dynamic MTs assume a role in bristle elongation, in a manner possibly related to their dynamic properties, then Klp10A RNAi bristles should show aberrant morphology. SEM analysis of adult Klp10A RNAi bristles revealed only mild defects at the bristle tip and no reduction in bristle length. However, during elongation, Klp10A RNAi bristles exhibited major abnormalities, including misguidance of shaft initiation sites. Thus, we suggest that dynamic MTs are important for establishing bristle polarity but are not necessary for bristle maintenance. This was also demonstrated by affecting only the dynamic MTs in bristles upon treatment with vinblastine (VB). VB has been reported to have different effects on bristle elongation according to the stage of induction: when injected into pupae prior to shaft initiation, VB causes significant elongation defects (Fei et al., 2002); however, incubation of elongating bristles with VB has no effect on continued elongation (Tilney et al., 2000). Thus, defects in polarity determination prior to shaft initiation lead to elongation defects, whereas destruction of dynamic MTs after polarity has no significant effect on bristle elongation.

Mutation of *ik2*, the *Drosophila ikkε* homolog, has been reported to affect polarized bristle morphology and elongation, leading to the appearance of short bristles with a swollen shaft segment and ectopic tip extensions (Bitan et al., 2010b; Dubin-Bar et al., 2008; Shapiro and Anderson, 2006). These morphological defects are related to MT disorganization during bristle elongation (Bitan et al., 2010b), actin stability defects due to an effect on DIAP1 (Oshima et al., 2006) and, as recently shown, interference with recycling endosome shuttling (Otani et al., 2011). We suggest that the high degree of disorganization of both stable and dynamic MTs in the swollen area of *ik2* mutant bristles, as seen in TEM longitudinal sections and by tracking EB1, could explain the elongation defects in these bristles. First, dynamic MT disorganization in the mutants leads to polarity determination defects, as demonstrated by the multiple misguided shaft extensions seen at the tip. Whereas Klp10A RNAi ectopic bristle extensions are pruned in a process that could be delayed by overexpression of DIAP1, *ik2* mutant ectopic extensions are not pruned and their durability could be related to the reported effect of Ik2 on DIAP1 (Kuranaga et al., 2006; Oshima et al., 2006). Second, we suggest that MT disorganization in *ik2* mutant bristles

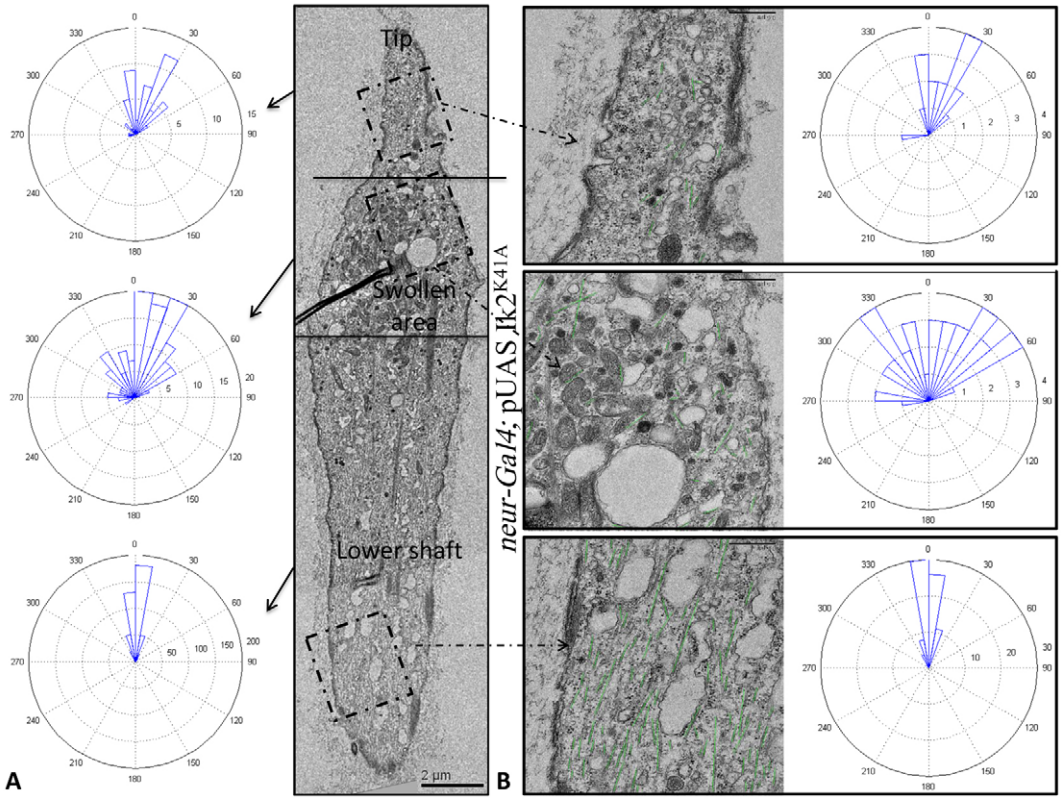

Fig. 8. Stable MTs are disoriented in the swollen and tip areas of *ik2* mutant bristles. (**A**) TEM micrographs of thin longitudinal sections through microchaete bristles expressing the *ik2* dominant-negative form (*neur*-Gal4; pUAS ik2^{K41A}) and rose diagrams of all stable MT orientations relative to the axis of the shaft in the different bristle regions. (**B**) Representative micrographs and their corresponding stable MT orientation rose diagrams. *ik2* mutant stable MTs run parallel to the axis of the shaft (in the range ±30°) in the lower shaft region, but are disoriented (in the range ±90°) in the swollen area and tip. Green lines indicate detected MTs. Scale bars: 2 µm in A; 0.5 µm in B.

interferes with the asymmetric distribution of cell components [as also shown by Bitan et al. (Bitan et al., 2010b)], leading to a failure to maintain bristle axial growth and to the concentration of vesicles and cell components in the swollen area, as was demonstrated by Otani et al. (Otani et al., 2011) and as seen in Fig. 8B.

We believe that *Drosophila* bristles offer a unique opportunity to gain new perspective into how cell elongation is achieved by coordination between two MT populations that are distinct in their polar characteristics and stability properties. Although dynamic MTs determine which way to grow, stable MTs provide the infrastructure to support the demanding process of cell elongation. Hence, each MT set is important for a different aspect of cell elongation, and their coordination with other cellular processes enables the establishment and maintenance of bristle shape.

Acknowledgements
We thank Thomas Hays, Tadashi Uemura, Masayuki Miura, VDRC Austria and the Bloomington Stock Center for generously providing fly strains; Gregory Guild, Ilan Davis, Richard Macintosh, Vladimir Galfend, Larisa Gever, Thomas Surrey and Clive Lloyd for productive discussions; Ofer Ovadia, Hagai Guterman and Ron Rotkof for help with statistical analysis; and Rina Jeger for microtome expertise.

Funding
This research was supported by the Israel Science Foundation [grant 968/10 to U.A.].

Competing interests statement
The authors declare no competing financial interests.

Supplementary material
Supplementary material available online at
http://dev.biologists.org/lookup/suppl/doi:10.1242/dev.076893/-/DC1

References
Baas, P. W. and Lin, S. (2011). Hooks and comets: the story of microtubule polarity orientation in the neuron. *Dev. Neurobiol.* **71**, 403-418.
Bainbridge, S. P. and Bownes, M. (1981). Staging the metamorphosis of Drosophila melanogaster. *J. Embryol. Exp. Morphol.* **66**, 57-80.
Bitan, A., Guild, G. M. and Abdu, U. (2010a). The highly elongated Drosophila mechanosensory bristle: a new model for studying polarized microtubule function. *Fly (Austin)* **4**, 246-248.
Bitan, A., Guild, G. M., Bar-Dubin, D. and Abdu, U. (2010b). Asymmetric microtubule function is an essential requirement for polarized organization of the Drosophila bristle. *Mol. Cell. Biol.* **30**, 496-507.
Dubin-Bar, D., Bitan, A., Bakhrat, A., Kaiden-Hasson, R., Etzion, S., Shaanan, B. and Abdu, U. (2008). The Drosophila IKK-related kinase (Ik2) and Spindle-F proteins are part of a complex that regulates cytoskeleton organization during oogenesis. *BMC Cell Biol.* **9**, 51.
Fei, X., He, B. and Adler, P. N. (2002). The growth of Drosophila bristles and laterals is not restricted to the tip or base. *J. Cell Sci.* **115**, 3797-3806.
Guild, G. M., Connelly, P. S., Vranich, K. A., Shaw, M. K. and Tilney, L. G. (2002). Actin filament turnover removes bundles from Drosophila bristle cells. *J. Cell Sci.* **115**, 641-653.
Ikegami, K. and Setou, M. (2010). Unique post-translational modifications in specialized microtubule architecture. *Cell Struct. Funct.* **35**, 15-22.
Kuo, C. T., Zhu, S., Younger, S., Jan, L. Y. and Jan, Y. N. (2006). Identification of E2/E3 ubiquitinating enzymes and caspase activity regulating Drosophila sensory neuron dendrite pruning. *Neuron* **51**, 283-290.
Kuranaga, E., Kanuka, H., Igaki, T., Sawamoto, K., Ichijo, H., Okano, H. and Miura, M. (2002). Reaper-mediated inhibition of DIAP1-induced DTRAF1 degradation results in activation of JNK in Drosophila. *Nat. Cell Biol.* **4**, 705-710.
Kuranaga, E., Kanuka, H., Tonoki, A., Takemoto, K., Tomioka, T., Kobayashi, M., Hayashi, S. and Miura, M. (2006). Drosophila IKK-related kinase regulates nonapoptotic function of caspases via degradation of IAPs. *Cell* **126**, 583-596.

Lees, A. D. and Waddington, C. H. (1942). The development of the bristles in normal and some mutant types of *Drosophila melanogaster*. *Proc. R. Soc. Lond. B* **131**, 87-110.
McIntosh, J. R. and Euteneuer, U. (1984). Tubulin hooks as probes for microtubule polarity: an analysis of the method and an evaluation of data on microtubule polarity in the mitotic spindle. *J. Cell Biol.* **98**, 525-533.
Mennella, V., Rogers, G. C., Rogers, S. L., Buster, D. W., Vale, R. D. and Sharp, D. J. (2005). Functionally distinct Kinesin-13 family members cooperate to regulate microtubule dynamics during interphase. *Nat. Cell Biol.* **7**, 235-245.
Mogensen, M. M., Tucker, J. B. and Stebbings, H. (1989). Microtubule polarities indicate that nucleation and capture of microtubules occurs at cell surfaces in Drosophila. *J. Cell Biol.* **108**, 1445-1452.
Oshima, K., Takeda, M., Kuranaga, E., Ueda, R., Aigaki, T., Miura, M. and Hayashi, S. (2006). IKK epsilon regulates F actin assembly and interacts with Drosophila IAP1 in cellular morphogenesis. *Curr. Biol.* **16**, 1531-1537.
Otani, T., Oshima, K., Onishi, S., Takeda, M., Shinmyozu, K., Yonemura, S. and Hayashi, S. (2011). IKKepsilon regulates cell elongation through recycling endosome shuttling. *Dev. Cell* **20**, 219-232.
Perdiz, D., Mackeh, R., Pous, C. and Baillet, A. (2011). The ins and outs of Tubulin acetylation: more than just a post-translational modification? *Cell Signal.* **23**, 763-771.
Rogers, G. C., Rogers, S. L., Schwimmer, T. A., Ems-McClung, S. C., Walczak, C. E., Vale, R. D., Scholey, J. M. and Sharp, D. J. (2004). Two mitotic kinesins cooperate to drive sister chromatid separation during anaphase. *Nature* **427**, 364-370.
Rosenbaum, J. (2000). Cytoskeleton: functions for tubulin modifications at last. *Curr. Biol.* **10**, R801-R803.
Rumpf, S., Lee, S. B., Jan, L. Y. and Jan, Y. N. (2011). Neuronal remodeling and apoptosis require VCP-dependent degradation of the apoptosis inhibitor DIAP1. *Development* **138**, 1153-1160.
Satoh, D., Sato, D., Tsuyama, T., Saito, M., Ohkura, H., Rolls, M. M., Ishikawa, F. and Uemura, T. (2008). Spatial control of branching within dendritic arbors by dynein-dependent transport of Rab5-endosomes. *Nat. Cell Biol.* **10**, 1164-1171.
Sawin, K. E. and Nurse, P. (1998). Regulation of cell polarity by microtubules in fission yeast. *J. Cell Biol.* **142**, 457-471.
Shapiro, R. S. and Anderson, K. V. (2006). Drosophila Ik2, a member of the I Kappa B kinase family, is required for mRNA localization during oogenesis. *Development* **133**, 1467-1475.
Silvanovich, A., Li, M. G., Serr, M., Mische, S. and Hays, T. S. (2003). The third P-loop domain in cytoplasmic Dynein heavy chain is essential for Dynein motor function and ATP-sensitive microtubule binding. *Mol. Biol. Cell* **14**, 1355-1365.
Tilney, L. G., Connelly, P. S., Vranich, K. A., Shaw, M. K. and Guild, G. M. (1998). Why are two different cross-linkers necessary for actin bundle formation in vivo and what does each cross-link contribute? *J. Cell Biol.* **143**, 121-133.
Tilney, L. G., Connelly, P. S., Vranich, K. A., Shaw, M. K. and Guild, G. M. (2000). Actin filaments and microtubules play different roles during bristle elongation in Drosophila. *J. Cell Sci.* **113**, 1255-1265.
Tilney, L. G., Connelly, P. S. and Guild, G. M. (2004). Microvilli appear to represent the first step in actin bundle formation in Drosophila bristles. *J. Cell Sci.* **117**, 3531-3538.
Williams, D. W. and Truman, J. W. (2005). Cellular mechanisms of dendrite pruning in Drosophila: insights from in vivo time-lapse of remodeling dendritic arborizing sensory neurons. *Development* **132**, 3631-3642.